

Self-consistent analysis of electron-phonon coupling parameters of graphene

Jessica L. McChesney,^{1,2} Aaron Bostwick,¹ Taisuke Ohta,^{1,2} Konstantin Emtsev,³ Thomas Seyller,³ Karsten Horn,² and Eli Rotenberg¹

¹Advanced Light Source, Lawrence Berkeley National Laboratory, Berkeley, California, USA

²Fritz-Haber-Institut der Max-Planck-Gesellschaft, Berlin, Germany

³Lehrstuhl für Angewandte Physik, Friedrich-Alexander Universität Erlangen-Nürnberg, Erlangen, Germany

(Dated: November 25, 2018)

We present a self-consistent analysis of the photoemission spectral function $A(\mathbf{k}, \omega)$ of graphene monolayers grown epitaxially on SiC(0001). New information derived from spectral intensity anomalies (in addition to linewidths and peak positions) confirms that sizeable kinks in the electronic dispersion at the Dirac energy E_D and near the Fermi level E_F arise from many-body interactions, not single-particle effects such as substrate bonding or extra bands. The relative electron-phonon scattering rate from phonons at different energy scales evolves with doping. The electron-phonon coupling strength is extracted and found to be much larger ($\sim 3.5 - 5$ times) than predicted.

PACS numbers: 73.21.-b, 71.38.-k, 73.22.-f, 79.60.-i

Many-body interactions in epitaxial graphene are interesting since graphene has been proposed for numerous device applications including high power electronics and novel device schemes [1, 2]. Full characterization of the electron scattering lifetime under a variety of conditions is therefore central to understanding the properties of such devices. Moreover, graphene is an excellent system for investigating theories of many-body interactions in two dimensions. First, it is straightforward to prepare high quality films, with intrinsic photoemission linewidths among the sharpest available for any material [3, 4]. Second, a large change in the carrier density of the order of $\pm 10^{13} e^-/\text{cm}^2$ can be achieved through applied voltage in a gated device [5, 6], or equivalently through chemical doping [7], suggesting a tunability of many-body effects for novel devices.

We have previously shown that the electron scattering lifetime of holes in n -doped graphene is dominated by a combination of ordinary Fermi liquid electron-hole pair ($e-h$) excitations, electron-phonon ($e-ph$) coupling, and electron-plasmon ($e-pl$) coupling [4]. Theoretical work has qualitatively confirmed the $e-h$ and $e-pl$ interpretation. Both Hwang *et al.* [8] and Polini *et al.* [9] have shown that the electron-plasmon interaction leads to an enhancement of the scattering rate, and a “ π -band mismatch”, where the lower and upper π bands are displaced from each other when projected through their crossing point at the Dirac energy E_D . These effects are similar to those seen in experiment, but are not predicted in single-particle theories, whereas they naturally arise from many-body interactions. Similarly, the dispersion of the bands near E_F is heavily modified, a fact which is ascribed conventionally to $e-ph$ coupling since the effects occur on a ~ 200 meV energy scale, corresponding to the phonon bandwidth of graphene [10, 11, 12].

Although the evidence for $e-ph$ and $e-pl$ coupling is strong, the existence of the $e-pl$ coupling and the quantitative estimate of the $e-ph$ coupling strength λ derived from the data remain controversial. First, as an alternate model to the $e-pl$ coupling, the bonding of graphene to the substrate induces a gap

at E_D [13, 14]. Alternative causes for a dispersion anomaly are the presence of defects or quantum size effects for islanded films [15, 16].

Second, a simple estimate of the coupling strength [17] gave $\lambda \sim 5$ times stronger than detailed calculations [10, 11, 18, 19]. This suggests a stronger role than predicted [18, 20] for π -band $e-ph$ coupling in superconductivity of graphite intercalation compounds (GICs) like CaC_6 . But the linear-band estimation method [17] was shown to overstate the coupling [21], and furthermore finite energy and momentum resolution was cited to explain at least part of the discrepancy [12].

Here we provide a self-consistent analysis of the experimental spectral function which makes no *a priori* assumptions about the bare bands, but assumes only non-violation of causality, approximate particle-hole symmetry, and a weak momentum- (\mathbf{k} -) dependence of the self energy. Self-consistency between model and data is demonstrated by a comparison of the scattering rates, dispersion energies, and the *absolute spectral intensity* – the latter having been not usually considered. From our analysis of the low doping regime ($n < 6 \times 10^{13} e^-/\text{cm}^2$), we find that: (i) key spectral features arise from many-body interactions, (ii) previous estimates of large $e-ph$ constant are confirmed, and (iii) the relative $e-ph$ coupling strength to multiple phonon modes is shown to be strongly doping-dependent. These results are a challenge to the present understanding of the carrier lifetimes in graphene.

The photoemission single particle spectral function is

$$A(\mathbf{k}, \omega) = \frac{|\text{Im}\Sigma(\mathbf{k}, \omega)|}{(\omega - \omega_b(\mathbf{k}) - \text{Re}\Sigma(\mathbf{k}, \omega))^2 + (\text{Im}\Sigma(\mathbf{k}, \omega))^2}, \quad (1)$$

where ω is the quasiparticle energy, $\omega_b(\mathbf{k})$ is the bare (unrenormalized) band, and $\Sigma(\mathbf{k}, \omega)$ is the complex quasiparticle self-energy, whose real and imaginary components are related by Hilbert transformation to satisfy causality. We seek to determine $\Sigma(\mathbf{k}, \omega)$ with no knowledge of the bare band $\omega_b(\mathbf{k})$ or the $\omega > 0$ spectral function, and subject to uncertainty due to experimental broadening. Once $\text{Re}\Sigma(\mathbf{k}, \omega)$ is determined, the

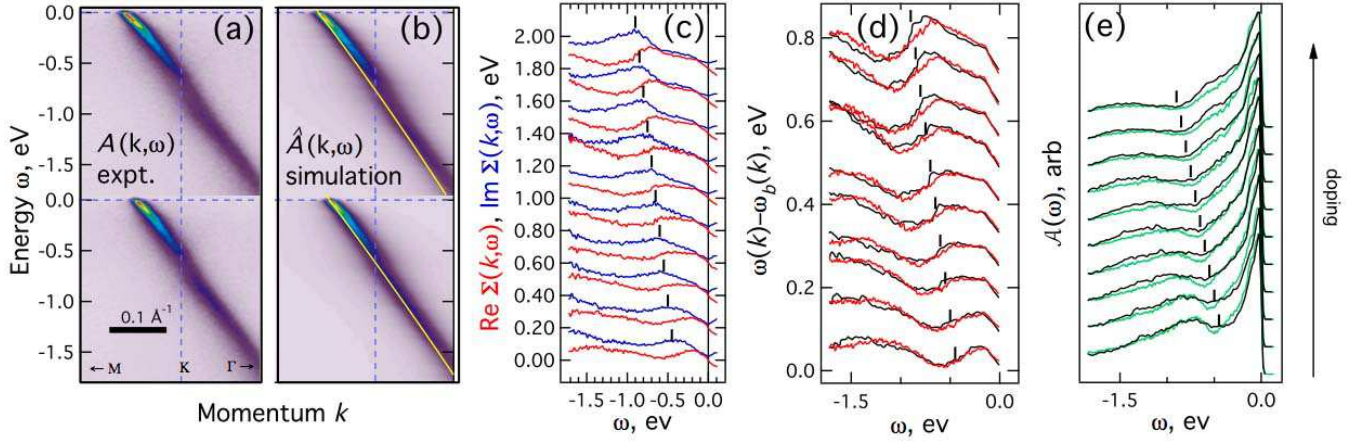


FIG. 1: (a) Experimental and (b) Simulated spectral functions $A(\mathbf{k}, \omega)$ for two dopings $n = 2.5, 3.9 \times 10^{13} \text{ e}^-/\text{cm}^2$. The dashed lines are E_F and the K point of the Brillouin zone, while the solid lines are the self-consistent bare bands. (c) Real and Imaginary parts of the self-energy (with 0.02 eV offset), (d) the difference between renormalized and bare bands, and (e) MDC amplitudes for experiment (red, green) and model (black) as a function of doping. The lowermost spectra correspond to as-grown graphene ($n = 1.2 \times 10^{13} \text{ e}^-/\text{cm}^2$), with doping increasing linearly for each subsequent spectrum, up to $n = 5.6 \times 10^{13} \text{ e}^-/\text{cm}^2$. The heavy lines in (c-e) mark the approximate Dirac energy E_D .

e - ph coupling constant λ is given by

$$\lambda = -\partial \text{Re} \Sigma(\mathbf{k}, \omega) / \partial k|_{\omega=0}. \quad (2)$$

In the usual analysis[22, 23], each momentum distribution curve (MDC) $A(\mathbf{k}, \omega=\text{const})$ is fitted to a Lorentzian and $A(\mathbf{k}, \omega)$ is thereby parametrized into three functions: the renormalized band dispersion $\omega(\mathbf{k})$, the Lorentzian width $\mathcal{W}(\omega)$, and $\mathcal{A}(\omega)$, the amplitude along $\omega(\mathbf{k})$. Provided the bare band is linear, $\text{Im} \Sigma(\mathbf{k}, \omega)$ is simply proportional to $\mathcal{W}(\omega)$ and the self-energy is easily found. However, if $\omega_b(\mathbf{k})$ is non-linear the problem is more difficult because of the non-trivial relationship between $\mathcal{W}(\omega)$ and $\text{Im} \Sigma(\mathbf{k}, \omega)$.

To solve the general problem, we apply an optimization approach similar to Kordyuk *et al.* [24]: From initial guesses for $\omega_b(\mathbf{k})$ and $\Sigma(\mathbf{k}, \omega)$, we calculate the simulated spectral function $\hat{A}(\mathbf{k}, \omega)$ and by MDC analysis parametrize it into three functions $\hat{\mathcal{W}}(\omega)$, $\hat{\mathcal{A}}(\omega)$, $\hat{\omega}(\mathbf{k})$. The self energy and bare band are iteratively refined in order to minimize the difference $\hat{\omega}(\mathbf{k}) - \omega(\mathbf{k})$ subject to the constraint $\hat{\mathcal{W}}(\omega) = \mathcal{W}(\omega)$. Agreement between simulated and experimental $\mathcal{A}(\omega)$ is left as a final check of the model. To reduce the number of free parameters, we use a quadratic bare band.

The experiments were performed on *in situ* grown samples at beamline 7.0 of the Advanced Light Source. Samples were prepared by epitaxial growth on SiC(0001) and doped with K atoms as described elsewhere [4, 7]. The instrumental broadenings were 25 meV and 0.01 \AA^{-1} , and the photon energy was 94 eV. The sample temperature was $\sim 20 \text{ K}$.

Fig. 1(a,b) shows two typical experimental spectral functions $A(\mathbf{k}, \omega)$ for different n -dopings of graphene, in comparison to simulated spectral functions $\hat{A}(\mathbf{k}, \omega)$. The latter were calculated using the optimized bare bands and $\Sigma(\mathbf{k}, \omega)$ shown in Fig. 1(b,c). We assumed particle-hole symmetry,

i.e. that $\text{Im} \Sigma(\mathbf{k}, \omega)$ is a strictly even function with respect to $\omega = 0$, implying $\text{Re} \Sigma(\mathbf{k}, 0) \rightarrow 0$. The intensity was scaled by a function linear with ω to account for the non-uniform sensitivity of the electron detector. Comparison of the quantity $(\omega(\mathbf{k}) - \omega_b(\mathbf{k}))$ derived from MDC fits of $A(\mathbf{k}, \omega)$ and $\hat{A}(\mathbf{k}, \omega)$ (Fig. 1(d)) shows excellent agreement, demonstrating self-consistency of our derived $\Sigma(\mathbf{k}, \omega)$, and confirming that deviations in the band dispersion indeed are fully described by quasiparticle scattering, and not details of the initial-state band structure. In particular, the energy gap at E_D [13, 14], if any, must be much smaller than the band renormalization by many-body interactions.

We stress that in our analysis the simulated and experimental spectral functions are treated on an equal footing with respect to temperature smearing at E_F and experimental broadening, both of which are included in our simulated $\hat{A}(\mathbf{k}, \omega)$. Therefore these uncertainties are in principle deconvolved out of our derived self-energies. Furthermore, we find that the calculated and experimental $\mathcal{A}(\omega)$ in excellent agreement (Fig. 1e), despite not being included in our optimization. This is a stringent test of the analysis, because as we now show, $\mathcal{A}(\omega)$ is highly sensitive to many-body interactions, perhaps more so than the MDC width and peak positions, a fact we can exploit to determine new information about e - ph coupling.

Fig. 2(a) shows simulated spectral functions for a band interacting with a single Einstein optical mode at $\omega_0 = 200 \text{ meV}$ using realistic experimental parameters, including a power-law scattering rate to simulate electron-electron interactions. The MDC amplitude function $\mathcal{A}(\omega)$ shows a relatively flat top down to ω_0 . Suppose we add additional weak scatterers at lower energy scales (Fig. 2(b,c)); how is the MDC analysis affected? Casual inspection of the $A(\mathbf{k}, \omega)$ images shows that scarcely any effect on the apparent dispersion or scattering rates can be observed with realistic broadening and limited statistics. However, the MDC amplitudes $\mathcal{A}(\omega)$ are strongly

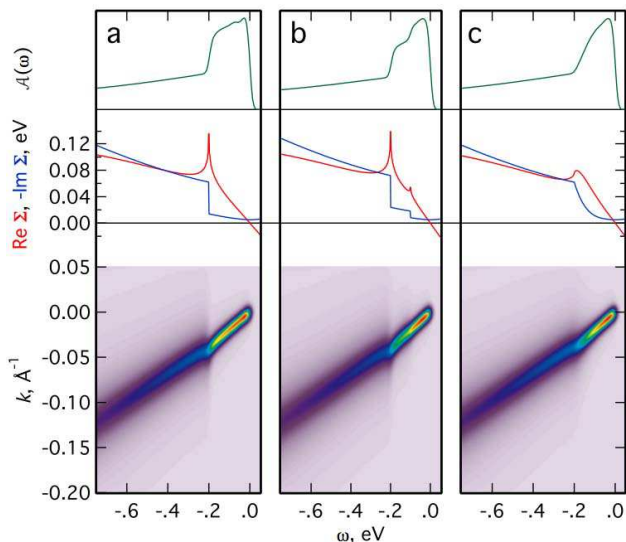


FIG. 2: Simulated spectral function and corresponding self-energy and fitted MDC amplitude $\mathcal{A}(\omega)$ for (a) a single Einstein phonon mode (b) the same, plus an additional Einstein mode at 100 eV of 20% relative strength, (c) a single mode at $\omega_0 = 200$ meV with additional modes decaying towards $\omega = 0$.

affected, with an easily visible shift of spectral weight from ω_0 towards E_F . This shows that $\mathcal{A}(\omega)$ can access information about weak or even sub-resolution features in the self-energy.

We believe that the evolution of such ‘hidden’ features with doping are necessary to explain the evolution of $\mathcal{A}(\omega)$ near E_F . Fig. 3 shows the measured $\mathcal{A}(\omega)$ as a function of doping. While all spectra show a break in slope around 200 meV, there is clearly an evolution from a merely prominent shoulder beginning around 200 meV to a flat top below E_F with increased doping. The simulations in Fig. 2 suggest that this shoulder is the dominant mode at all dopings, but its strength increases relative to the lower energy modes with doping. Such a relative evolution of the e - ph coupling with different phonon modes has not been predicted by theory.

We close by discussing how the self-energy and experimentally derived e - ph coupling constant λ compares to recent calculations. The globally optimized self-energies in Fig. 1 do not fit perfectly well near E_F , since the quadratic bare band does not fit the data perfectly over all energies. To achieve a more accurate $\Sigma(\mathbf{k}, \omega)$ near E_F , we have analyzed the data in a smaller energy region, shown in Fig. 4(a) for a sample with $E_F - E_D \sim .65$ eV.

The simulated $\hat{A}(\mathbf{k}, \omega)$ and the derived self-energy $\Sigma(\mathbf{k}, \omega)$ and bare band $\omega_b(\mathbf{k})$ are shown in Fig. 4(b, d). Good agreement between measured and simulated $\omega(\mathbf{k})$, $\mathcal{W}(\omega)$, and $\mathcal{A}(\omega)$ are demonstrated in Fig. 4(e-g). For comparison, in Fig. 4(c) we show the spectral function calculated from the predicted e - ph $\Sigma(\mathbf{k}, \omega)$ from Ref. [11]. Both the experimental and the predicted $A(\mathbf{k}, \omega)$ were modeled with a .028 eV offset to $\text{Im}\Sigma(\mathbf{k}, \omega)$ to take care of the background defect scattering rate. Although in excellent qualitative agreement, the theoret-

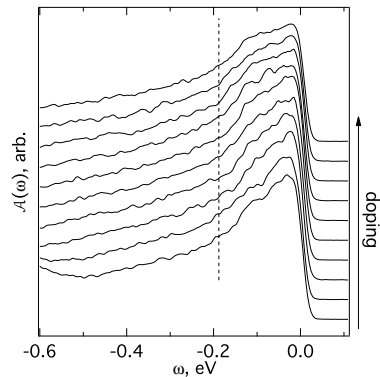


FIG. 3: Experimental $\mathcal{A}(\omega)$ for the same samples as in Fig. 1. The onset position of the phonon kink at ~ 200 eV is shown by the dashed line.

ical self-energies are much smaller than those measured (see comparison in Fig. 4(d)), and hence the kink, scattering rates, and the abrupt increase in the spectral amplitude $\mathcal{A}(\omega)$ are not well-reproduced (Fig. 4(e-g)). This conclusion is not affected by experimental broadening as proposed in [12] because the same discrepancy appears in both the optimized self-energies (from which the broadening is essentially deconvolved, see Fig. 4(d)) as well as from the apparent self-energy derived from both experiment and broadened theory (Fig. 4(e-f)). Furthermore the disagreement in $\mathcal{A}(\omega)$ is practically unaffected by our experimental broadening.

The discrepancy in λ ranges from a factor of 3.5 to 5 times larger than predictions for e - ph coupling [10, 11, 12], the lower estimate found by scaling the predicted real and imaginary parts of $\Sigma(\mathbf{k}, \omega)$ to match the experimental functions, and the upper estimate by applying Eq. 2 to the two $\text{Re}\Sigma(\mathbf{k}, \omega)$ functions in Fig. 4(d) [25]. If some of the scattering is attributed to electron-electron coupling near E_F (which rises as $\sim \omega^2$) [9] then this would act to reduce the derived e - ph coupling constant, however, the e - e contribution to $\text{Im}\Sigma(\mathbf{k}, \omega)$ is predicted to be very weak (around .004 eV at $\omega = 200$ meV) [26], and it cannot explain the sharp kink at the phonon energy scale [8, 9].

Why is the apparent e - ph coupling so large? First, it could be due to coupling to some other mode (e.g. magnon) at similar energy scale, although such a mode has not been observed or even predicted. It cannot be due to coupling to substrate phonons, because the SiC phonon modes are at lower energies than the observed kink. Furthermore there is a carbon-rich, graphene-like buffer layer between graphene and SiC [27], whose coupling to the graphene electrons would also have to be anomalously high to explain the results.

The presence of our dopant K atoms cannot explain the large coupling: first, because of the apparent strong coupling even in our as-grown films, and second, because K vibrations are at too low an energy to explain the kink (although they might contribute in principle to the lower-energy modes suggested in our self-energy in Fig. 4(d)). Also, the very minute

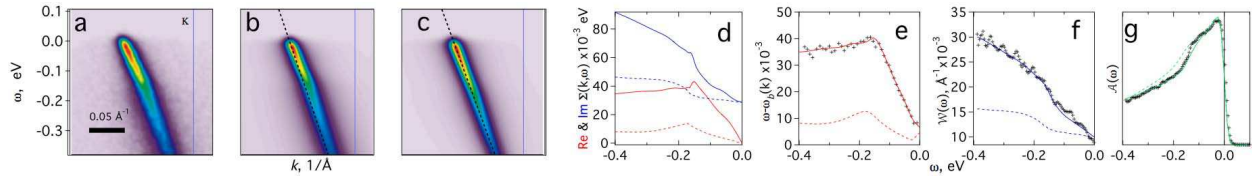


FIG. 4: Spectral function of graphene for $n = 3.4 \times 10^{13} \text{ e}^-/\text{cm}^2$ (a) experimental $A(\mathbf{k}, \omega)$, (b) optimized model $\hat{A}(\mathbf{k}, \omega)$, (c) model $\hat{A}(\mathbf{k}, \omega)$ using self energy by Park *et al.* (d-g) the self-energies, dispersions, MDC widths, and $\mathcal{A}(\omega)$ are compared for the results of the MDC analysis of $A(\mathbf{k}, \omega)$ (markers) and the models, with (solid, dashed) lines corresponding to (b, c).

amount of K atoms ($\sim .06$ per graphene unit cell at our highest doping) makes its presence unlikely to cause the effect we see. Lastly, there is a small rippling of graphene on SiC [28]. Although a local curvature can enhance the e - ph coupling [29], the curvature in our films is too small to have a significant effect.

Our findings lead to three possibilities, first, that λ for graphene is anomalously strong, second, that there is anomalously strong scattering from something other than phonons (such as defects, or e - e scattering) on a similar energy scale, or third, there is a mutual interplay of interactions that leads to an enhanced scattering rate overall. Noting that the peak near E_D in $\text{Im}\Sigma$ due to plasmon scattering is broadened and shifted towards E_F in our experiment relative to calculations [8, 9], such an interplay is conceivable.

We acknowledge C. W. Park, F. Guistino, S. G. Louie, M. L. Cohen, M. Polini, A. H. MacDonald, T. Deveraux, M. Calandra and F. Mauri for discussions. This work and the ALS are supported by the Director, Office of Science, Office of Basic Energy Sciences, Materials Sciences Division, of the U.S. DOE under Contract No. DE-AC03-76SF00098 at LBNL. J.M., T.O., and K.H. were supported by the Max Planck Society. TS and KE acknowledge support by the DFG through SE1087/5-1 and by the Erlangen Cluster of Excellence "Engineering of Advanced Materials". (<http://www.eam.uni-erlangen.de>).

[1] A. K. Geim and K. S. Novoselov, *Nat Mater* **6**, 183 (2007).
 [2] C. Berger, Z. Song, X. Li, X. Wu, N. Brown, C. Naud, D. Mayou, T. Li, J. Hass, A. Marchenkov, et al., *Science* **312**, 1191 (2006).
 [3] I. Forbeaux, J. M. Themlin, and J. M. Debever, *Phys. Rev. B* **58**, 16396 (1998).
 [4] A. Bostwick, T. Ohta, T. Seyller, K. Horn, and E. Rotenberg, *Nat Phys* **3**, 36 (2007).
 [5] K. S. Novoselov, E. McCann, S. V. Morosov, V. Fal'ko, M. I. Katsnelson, U. Zeitler, D. Jiang, F. Schedin, and A. K. Geim, *Nature* **438**, 192 (2005).
 [6] Y. Zhang, Y. W. Tan, H. L. Stormer, and P. Kim, *Nature* **438**, 201 (2005).
 [7] T. Ohta, B. Bostwick, T. Seyller, K. Horn, and E. Rotenberg,

Science **313**, 951 (2006).
 [8] E. H. Hwang and S. DasSarma, *Phys. Rev. B* **77**, 081412(R) (2008).
 [9] M. Polini, R. Asgari, G. Borghi, Y. Barlas, T. Pereg-Barnea, and A. H. MacDonald, *Phys. Rev. B* **77**, 081411(R) (2008).
 [10] W.-K. Tse and S. DasSarma, *Phys. Rev. Lett.* **99**, 236802 (2007).
 [11] C.-H. Park, F. Giustino, M. L. Cohen, and S. G. Louie, *Phys. Rev. Lett.* **99**, 086804 (2007).
 [12] M. Calandra and F. Mauri, *Phys. Rev. B* **76**, 205411 (2007).
 [13] S. Y. Zhou, G. H. Gweon, A. V. Fedorov, P. N. First, W. A. de Heer, D. H. Lee, F. Guinea, A. H. Castro Neto, and A. Lanzara, *Nat. Mater.* **6**, 770 (2007).
 [14] S. Kim, J. Ihm, H. J. Choi, and Y.-W. Son, *Phys. Rev. Lett.* **100**, 176802 (2008).
 [15] E. Rotenberg, A. Bostwick, T. Ohta, J. L. McChesney, T. Seyller, and K. Horn, *Nat. Mater.* **7**, 258 (2008).
 [16] S. Y. Zhou, D. A. Siegel, A. V. Federov, F. El Gabaly, A. K. Schmid, A. H. Castro Neto, D. H. Lee, and A. Lanzara, *Nat. Mater.* (2008).
 [17] A. Bostwick, T. Ohta, J. L. McChesney, T. Seyller, K. Horn, and E. Rotenberg, *Solid State Communications* **143**, 63 (2007).
 [18] M. Calandra and F. Mauri, *Phys. Rev. Lett.* **95**, 237002 (2005).
 [19] M. Calandra and F. Mauri, *physica status solidi (b)* **243**, 3458 (2006).
 [20] J. S. Kim, L. Boeri, R. K. Kremer, and F. S. Razavi, *Phys. Rev. B* **74**, 214513 (2006).
 [21] C.-H. Park, F. Giustino, J. L. McChesney, A. Bostwick, T. Ohta, E. Rotenberg, M. L. Cohen, and S. G. Louie, *Phys. Rev. B* **77**, 113410 (2008).
 [22] A. Damascelli, Z. Hussain, and Z. X. Shen, *Review of Modern Physics* **75**, 473 (2003).
 [23] A. Kaminski and H. M. Fretwell, *New Journal of Physics* **7**, 98 (2005), 1367-2630.
 [24] A. A. Kordyuk, S. V. Borisenko, A. Koitzsch, J. Fink, M. Knupfer, and H. Berger, *Phys. Rev. B* **71**, 214513 (2005).
 [25] Calculation over a 100 meV binding energy range near E_F .
 [26] The quasiparticle peak at $\omega=0.2$ eV corresponds to $\omega/(E_F - E_D) = 0.3$, and normalized momentum $k/k_F \sim 0.75$. The predicted $\text{Im}\Sigma/(E_F - E_D) \sim .0059$ is read from Fig. 4 of Ref. [9], or $\text{Im}\Sigma \sim .0038$ eV.
 [27] K. V. Emtsev, F. Speck, T. Seyller, L. Ley, and J. D. Riley, *Phys. Rev. B* **77**, 155303 (2008).
 [28] F. Varchon, P. Mallet, J. Y. Veuillen, and L. Magaud, *Phys. Rev. B* **77**, 235412 (2008).
 [29] V. H. Crespi, *Physical Review B* **60**, 100 (1999).